

# $A^*$ for Graphs of Convex Sets

Kaarthik Sundar<sup>1</sup> and Sivakumar Rathinam<sup>2</sup>

**Abstract**—We present a novel algorithm that fuses the existing convex-programming based approach with heuristic information to find optimality guarantees and near-optimal paths for the Shortest Path Problem in the Graph of Convex Sets (SPP-GCS). Our method, inspired by  $A^*$ , initiates a best-first-like procedure from a designated subset of vertices and iteratively expands it until further growth is neither possible nor beneficial. Traditionally, obtaining solutions with bounds for an optimization problem involves solving a relaxation, modifying the relaxed solution to a feasible one, and then comparing the two solutions to establish bounds. However, for SPP-GCS, we demonstrate that reversing this process can be more advantageous, especially with Euclidean travel costs. In other words, we initially employ  $A^*$  to find a feasible solution for SPP-GCS, then solve a convex relaxation restricted to the vertices explored by  $A^*$  to obtain a relaxed solution, and finally, compare the solutions to derive bounds. We present numerical results to highlight the advantages of our algorithm over the existing approach in terms of the sizes of the convex programs solved and computation time.

## I. INTRODUCTION

The Shortest Path Problem (SPP) is one of the most important and fundamental problems in discrete optimization [1]–[3]. Given a graph, the SPP aims to find a path between two vertices in the graph such that the sum of the cost of the edges in the path is minimized. In this paper, we concern ourselves with a generalization of the SPP, recently introduced in [4], where each vertex is associated with a convex set and the cost of the edge joining any two vertices depends on the choice of the points selected from each of the respective convex sets. In this generalization, referred to as the *Shortest Path Problem in the Graph of Convex Sets* (SPP-GCS) [4], the objective is to find a path and choose a point from each convex set associated with the vertices in the path such that the sum of the cost of the edges in the path is minimized (Fig. 1). The SPP-GCS naturally arises in several applications including motion planning of robots [5], [6], planning problems with neighborhoods [7], [8] and control of hybrid systems [4]. Numerical and experimental results [4]–[6] have also shown that collision-free trajectories can be reliably designed using solutions to SPP-GCS in high-dimensional complex environments.

SPP-GCS reduces to the standard SPP if the point to be selected from each convex set is given. Also, SPP-GCS reduces to a relatively easy-to-solve convex optimization problem if the path is given. Selecting an optimal point in each set, as well as determining the path, makes the SPP-GCS NP-Hard in the general case [4]. Brute force algorithms, which find all feasible paths from the origin to the destination and then selects a path that yields the shortest length, may not be

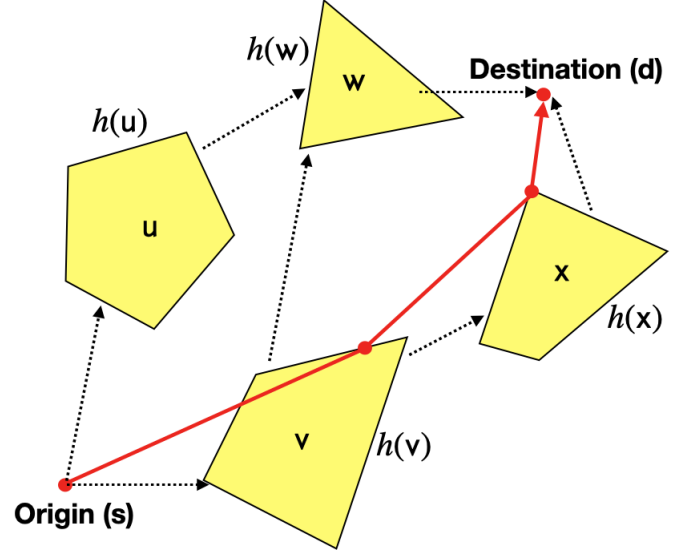


Fig. 1: Illustration of the SPP-GCS. The graph has six vertices, with the origin and the destination corresponding to singleton sets. The dotted lines represent the edges in the graph. Each vertex  $t$  in the graph is associated with a heuristic value  $h(t)$ , which denotes an underestimate of the cost to go from any point in the convex set corresponding to  $t$  to the destination. Note that,  $h(d) := 0$ . A feasible path for SPP-GCS is shown with solid (red) line segments.

computationally feasible<sup>1</sup>. Another possible method for finding the optimum is to formulate the SPP-GCS as a Mixed Integer Conic Program (MICP) [4]. However, solving this MICP to optimality can also be practically infeasible<sup>2</sup>. Therefore, we are interested in algorithms that can generate lower and upper bounds for the SPP-GCS. A lower bound can be obtained by solving a relaxation of the SPP-GCS, and an upper bound can be obtained by computing the length of a feasible solution to the SPP-GCS. Optimality guarantees can then be obtained by comparing the bounds. One of the key results in [4] is that there is a convex relaxation of an MILP for SPP-GCS that is not only computationally feasible to solve but also yields tight lower bounds or underestimates for the length of the shortest path for the SPP-GCS. Simple rounding-based heuristics [4] can then be applied to quickly convert the lower bounding

<sup>1</sup>The number of feasible paths heavily relies on the structure of the graph; for some graphs, this number could grow exponentially with the size of the graph.

<sup>2</sup>For example, the MICP (9)-(17) implemented in Gurobi [9], with a time limit of 7200 seconds, is not able to find optimal or near-optimal solutions (within a 0.5% optimality gap) for 2D maps 5 and 6, as well as the two 3D maps considered in this paper. In fact, for the 3D maps, the optimality gap after 7200 seconds of CPU time is still in the order of ten thousand.

1. Los Alamos Research Laboratory, New Mexico, 88220, USA.

2. Texas A&M University, College Station, TX 77843, USA.

solutions into feasible paths for the SPP-GCS.

Solving SPP-GCS and its relaxation is important in the context of robot motion planning because it allows for obtaining optimality guarantees for some fundamental robot motion planning problems (*e.g.* the SPP in 3D with obstacles [10], [11]) by partitioning the free configuration space of a robot into a collection of convex sets and then solving the SPP-GCS on the partition. However, partitioning the entire free space, especially in 3D or higher dimensions, can result in a large number of convex sets and a convex relaxation that is still computationally challenging to solve. Our motivation for this paper is to explore faster methods for solving convex relaxations of the SPP-GCS, with the ultimate goal of developing efficient approaches to generate optimality guarantees for hard robot motion planning problems.

One way to develop fast algorithms for an optimization problem is to incorporate heuristic information into the search process. The celebrated  $A^*$  algorithm [12] accomplishes this for the SPP. The consistent and more informed the heuristic information is, the fewer the number of expanded vertices in the  $A^*$  search process [12].

The objective of this paper is to propose a new algorithm that combines the existing convex-programming based approach in [4] with heuristic information to find optimality guarantees and near-optimal paths for SPP-GCS. We refer to the proposed algorithm as  $A^*$  for Graphs of Convex Sets ( $A^*$ -GCS). Just like in  $A^*$  [12], we assume that each vertex (or each convex set) has an associated heuristic cost to go from the vertex to the destination (Fig. 1).  $A^*$ -GCS follows the spirit of  $A^*$  and initiates a best-first-like search procedure from a designated set  $S$  (containing the origin) and iteratively builds on it until further growth is neither possible nor beneficial. A key step in  $A^*$ -GCS lies in the way we grow  $S$  in each iteration. To choose vertices for addition to  $S$ , we employ a relaxed solution to a generalization of the SPP-GCS that encompasses the vertices in  $S$  and their neighbors. In the special case when the convex sets reduce to singletons and the heuristic information is consistent,  $A^*$ -GCS reduces to  $A^*$ . On the other hand, if heuristic information is not available,  $A^*$ -GCS reduces to iteratively solving a convex relaxation of SPP-GCS until the termination conditions are satisfied.

Unlike  $A^*$ , which typically starts its search from a closed set  $S$  containing only the origin,  $A^*$ -GCS can start its search from any set  $S$  as long as it induces a cut — meaning  $S$  contains the origin but not the destination. In this paper, we consider two initial choices for  $S$  to start the search: one where  $S$  only contains the origin, and another where  $S$  contains vertices informed by applying  $A^*$  to a representative point (*e.g.* the centroid) from each convex set. One of the key insights we infer from the numerical results with Euclidean travel costs is that the second choice where  $A^*$ -GCS starts with the set  $S$  informed by  $A^*$  provides the best trade-off between achieving good quality bounds and smaller computation times. In general,  $A^*$ -GCS works on relatively smaller convex programs because its vertices are informed by the  $A^*$  algorithm, which only explores a subset of vertices in the graph. This leads to reduced computation times compared to solving a convex relaxation on the entire graph.

Typically, to obtain optimality guarantees for an optimization problem, we solve a relaxation of the problem, modify the relaxed solution to obtain a feasible solution, and then compare the two solutions to establish bounds. This is the approach followed in [4]. *In this paper, we demonstrate that reversing this process can be more effective in obtaining bounds for the SPP-GCS, especially with Euclidean travel costs. Specifically, we first implement  $A^*$  using a representative point from each convex set to obtain a feasible solution. We then solve a convex program on subsets of vertices informed by  $A^*$  to find a relaxed solution and subsequently compare the solutions.* In hindsight, this approach seems natural; since  $A^*$  quickly finds good feasible solutions for the SPP-GCS with a heuristic, it is reasonable to expect that good lower bounds can also be found in the neighborhood of the vertices visited by  $A^*$ , based on the strong formulation in [4].

After presenting the algorithms with theoretical bounding guarantees, we provide extensive computational results on the performance of  $A^*$ -GCS for instances derived from mazes, axis-aligned bars and 3D villages. While these numerical results clearly illustrate the benefits of  $A^*$ -GCS for travel costs based on Euclidean distances, we do not claim that the proposed approach is superior to directly solving the SPP-GCS for every instance. Nevertheless, the proposed approach is the first of its kind for SPP-GCS and opens a new avenue for research into related problems.

## II. PROBLEM STATEMENT

Let  $V$  denote a set of vertices, and  $E$  represent a set of directed edges joining vertices in  $V$ . Let each vertex  $v \in V$  be associated with a non-empty, compact convex set  $\mathcal{X}_v \subset \mathbb{R}^n$ . Given vertices  $u, v \in V$ , the cost of traveling the edge  $e = (u, v)$  from  $u$  to  $v$  depends on the choice of the points in the sets  $\mathcal{X}_u$  and  $\mathcal{X}_v$ . Specifically, given points  $x_u \in \mathcal{X}_u$  and  $x_v \in \mathcal{X}_v$ , let  $cost(x_u, x_v)$  denote the travel cost of edge  $e = (u, v)$ . In this paper, we set  $cost(x_u, x_v)$  to be equal to the Euclidean distance between the points  $x_u$  and  $x_v$ , *i.e.*,  $cost(x_u, x_v) := \|x_u - x_v\|_2$ .

Any path in the graph  $(V, E)$  is a sequence of vertices  $(v_1, v_2, \dots, v_k)$  for some positive integer  $k$  such that  $v_i \in V$ ,  $i = 1, \dots, k$  and  $(v_i, v_{i+1}) \in E$ ,  $i = 1, \dots, k - 1$ . Given a path  $\mathcal{P} := (v_1, v_2, \dots, v_k)$  and points  $x_{v_i} \in \mathcal{X}_{v_i}$ ,  $i = 1, \dots, k$ , the cost of traveling  $\mathcal{P}$  is defined as  $\sum_{i=1}^{k-1} cost(x_{v_i}, x_{v_{i+1}})$ . Given an origin  $s \in V$  and destination  $d \in V$ , the objective of the SPP-GCS is to find a path  $\mathcal{P} := (v_1, v_2, \dots, v_k)$  and points  $x_{v_i} \in \mathcal{X}_{v_i}$ ,  $i = 1, \dots, k$ , such that  $v_1 = s$ ,  $v_k = d$ , and the cost of traveling  $\mathcal{P}$  is minimized. The optimal cost for SPP-GCS is denoted as  $C_{opt}(s, d)$ .

## III. GENERALIZATION OF SPP-GCS AND ITS RELAXATION

We first introduce some notations specific for  $A^*$ -GCS. For each vertex  $v \in V$ , let  $h(v)$  denote an underestimate to the optimal cost for the SPP-GCS from  $v$  to  $d$ , *i.e.*,  $h(v) \leq C_{opt}(v, d)$ . We refer to such underestimates as admissible (just like in  $A^*$  [12]). Note that for the destination  $d$ , the underestimate  $h(d) = 0$ . We also refer to  $h(\cdot)$  as a heuristic

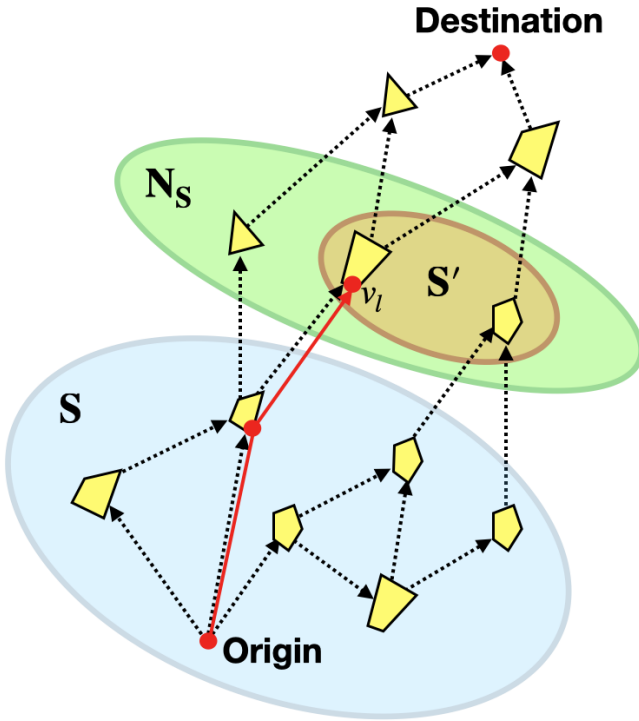


Fig. 2: Setup in the SPP\*-GCS showing the cut-set  $S$ , and subsets  $N_S$  and  $S'$ .  $N_S$  contains all the vertices in  $V \setminus S$  that are adjacent to  $S$ , and  $S'$  is any nonempty subset of  $N_S$ . A feasible path for SPP\*-GCS is shown with solid (red) line segments.

function for  $A^*$ -GCS. Given any  $S \subset V$ , let  $N_S$  denote the set of all the vertices in  $V \setminus S$  that are adjacent to at least one vertex in  $S$ , i.e.  $N_S := \{v : u \in S, v \notin S, (u, v) \in E\}$ .  $N_S$  is also referred to as the neighborhood of  $S$ .

Now, consider a closely related problem to SPP-GCS referred to as SPP\*-GCS defined on non-empty subsets  $S \subset V$  and  $S' \subseteq N_S$  such that  $s \in S$  and  $d \notin S$ . We will refer to any set  $S \subset V$  that satisfies  $s \in S$  and  $d \notin S$  as a *cut-set* in this paper (refer to Fig. 2). We will restrict our attention to the vertices in  $\bar{V} := S \cup S'$  and the edges in  $\bar{E} := \{(u, v) : u \in S, v \in \bar{V}, (u, v) \in E\}$ . The objective of SPP\*-GCS is to find a terminal vertex  $v_l$ , a path  $\mathcal{P}_g := (v_1, v_2, \dots, v_l)$  in the graph  $(\bar{V}, \bar{E})$  and points  $x_{v_i} \in \mathcal{X}_{v_i}$ ,  $i = 1, \dots, l$  such that  $v_1 = s$ ,  $v_l \in S'$ , and the sum of the cost of traveling  $\mathcal{P}_g$  and the heuristic cost,  $h(v_l)$ , is minimized. The optimal cost for SPP\*-GCS is denoted as  $C_{opt}^*(S, S')$ . The following Lemma shows the relationship between SPP\*-GCS and SPP-GCS.

**Lemma 1.** *SPP\*-GCS is a generalization of SPP-GCS.*

*Proof:* Without loss of generality, we assume there is at least one feasible path from  $s$  to  $d$  in the graph  $(V, E)$ . Therefore, if  $S := V \setminus \{d\}$ , then  $N_S := \{d\}$ . Hence,  $C_{opt}^*(V \setminus \{d\}, \{d\}) = C_{opt}(s, d)$  as  $h(d) = 0$ . ■

**Remark 1.** *In the special case when the convex sets reduce to singletons, SPP\*-GCS simplifies to a variant of a SPP where the objective is to find a path from the origin to a vertex*

$v_l$  in  $S'$  such that the sum of the cost to arrive at  $v_l$  and the heuristic cost  $h(v_l)$  is minimized. This variant of SPP is exactly the optimization problem solved during each iteration of  $A^*$ , where  $S$  represents the closed set and  $S'$  denotes the open set. While a simple best-first search is sufficient to solve this problem in  $A^*$ , such methods may not directly extend and produce good solutions for SPP\*-GCS.

#### A. Non-Linear Program for SPP\*-GCS

To formulate SPP\*-GCS, we use two sets of binary variables to specify the path and a set of continuous variables to choose the points from the convex sets corresponding to the vertices in the path. The first set of binary variables, denoted by  $y_{uv}$  for  $(u, v) \in \bar{E}$ , determines whether the edge  $(u, v)$  is selected in a solution to the SPP\*-GCS. Here,  $y_{uv} = 1$  implies that the edge  $(u, v)$  is chosen, while  $y_{uv} = 0$  implies the opposite. The second set of variables, denoted by  $\alpha_v$  for  $v \in S'$ , determines whether the vertex  $v$  is selected as a terminal or not. The continuous variable  $x_u$  for  $u \in \bar{V}$  specifies the point chosen in the convex set corresponding to vertex  $u$ . For any vertex  $u \in \bar{V}$ , let  $\delta^+(u)$  be the subset of all the edges in  $\bar{E}$  leaving  $u$ , and let  $\delta^-(u)$  be the subset of all the edges in  $\bar{E}$  coming into  $u$ . The non-linear program for SPP\*-GCS is as follows:

$$C_{opt}^*(S, S') := \min \sum_{(u,v) \in \bar{E}} \text{cost}(x_u, x_v) y_{uv} + \sum_{v \in S'} \alpha_v h(v) \quad (1)$$

$$\sum_{v \in S'} \alpha_v = 1 \quad (2)$$

$$\sum_{v \in \bar{V}} y_{sv} = 1 \quad (3)$$

$$\sum_{(u,v) \in \bar{E}} y_{uv} = \alpha_v \text{ for } v \in S' \quad (4)$$

$$\sum_{(u,v) \in \delta^-(v)} y_{uv} = \sum_{(v,u) \in \delta^+(v)} y_{vu} \text{ for } v \in S \setminus \{s\} \quad (5)$$

$$x_u \in \mathcal{X}_u \text{ for all } u \in \bar{V} \quad (6)$$

$$y_{uv} = \{0, 1\} \text{ for all } (u, v) \in \bar{E} \quad (7)$$

$$\alpha_v = \{0, 1\} \text{ for all } v \in S' \quad (8)$$

Constraints (2) state that exactly one vertex in  $S'$  must be chosen as a terminal. Constraints (3)-(5) state the standard flow constraints for a path from  $s$  to a terminal in  $S'$ . Constraint (6) states that for any vertex  $u \in \bar{V}$ , its corresponding point must belong to  $\mathcal{X}_u$ . The main challenge in solving the above formulation arises from the multiplication of the travel costs and the binary variables in (1). To address this challenge, we follow the approach in [4] and reformulate SPP\*-GCS as a Mixed Integer Convex Program (MICP) in the next subsection.

#### B. MICP for SPP\*-GCS

In this paper, as we are only dealing with travel costs derived from Euclidean distances, the objective in (1) can be re-written as:

$$\begin{aligned}
C_{opt}^*(S, S') &= \min \sum_{(u,v) \in \bar{E}} \|x_u - x_v\|_2 y_{uv} + \sum_{v \in S'} \alpha_v h(v) \\
&= \min \sum_{(u,v) \in \bar{E}} \|x_u y_{uv} - x_v y_{uv}\|_2 + \sum_{v \in S'} \alpha_v h(v).
\end{aligned}$$

In [4], the bi-linear terms  $x_u y_{uv}$  and  $x_v y_{uv}$  in the objective above are replaced with new variables, and the constraints in (5),(6) are transformed to form a MICP. Before we present the MICP corresponding to SPP\*-GCS, we first need to define the *perspective* of a set. The perspective of a compact, convex set  $\mathcal{X} \subset \mathbb{R}^n$  is defined as  $\bar{\mathcal{X}} := \{(x, \lambda) : \lambda \geq 0, x \in \lambda \mathcal{X}\}$ . Now, let  $x_u y_{uv} = z_{uv}$  and  $x_v y_{uv} = z'_{uv}$  for all  $(u, v) \in \bar{E}$ . By following the same procedure outlined in [4], we derive a Mixed-Integer Convex Program (MICP) for the SPP\*-GCS as follows:

$$\min \sum_{(u,v) \in \bar{E}} \|z_{uv} - z'_{uv}\|_2 + \sum_{v \in S'} \alpha_v h(v) \quad (9)$$

$$\sum_{v \in S'} \alpha_v = 1 \quad (10)$$

$$\sum_{v \in \bar{V}} y_{sv} = 1 \quad (11)$$

$$\sum_{(u,v) \in \bar{E}} y_{uv} = \alpha_v \text{ for } v \in S' \quad (12)$$

$$\sum_{(u,v) \in \delta^-(v)} (z'_{uv}, y_{uv}) = \sum_{(v,u) \in \delta^+(v)} (z_{vu}, y_{vu}) \text{ for } v \in S \setminus \{s\} \quad (13)$$

$$(z_{uv}, y_{uv}) \in \bar{\mathcal{X}}_u \text{ for all } u \in \bar{V}, (u, v) \in \bar{E} \quad (14)$$

$$(z'_{uv}, y_{uv}) \in \bar{\mathcal{X}}_v \text{ for all } v \in \bar{V}, (u, v) \in \bar{E} \quad (15)$$

$$y_{uv} = \{0, 1\} \text{ for all } (u, v) \in \bar{E} \quad (16)$$

$$\alpha_v = \{0, 1\} \text{ for all } v \in S' \quad (17)$$

**Lemma 2.** *The MICP formulation in (9)-(17) for the SPP\*-GCS has an optimal value equal to  $C_{opt}^*(S, S')$ .*

*Proof:* This result follows the same proof as Theorem 5.7 in [4]. ■

We now arrive at the relaxation used in our algorithms:

### Convex Relaxation for SPP\*-GCS

$$R_{opt}^*(S, S') = \min \sum_{(u,v) \in \bar{E}} \|z_{uv} - z'_{uv}\|_2 + \sum_{v \in S'} \alpha_v h(v)$$

subject to the constraints in (10)-(15) and,

$$\begin{aligned}
0 \leq y_{uv} \leq 1 \text{ for all } (u, v) \in \bar{E}, \\
0 \leq \alpha_v \leq 1 \text{ for all } v \in S'. \quad (18)
\end{aligned}$$

**Remark 2.** *In the special case when the convex sets reduce to singletons, the relaxation of SPP\*-GCS in (18) can be re-*

*formulated as a linear program with a coefficient matrix that is Totally Uni-Modular (TUM) [13], and as a result, its extreme points are optimal solutions for the SPP\*-GCS.*

## IV. A\*-GCS

A\*-GCS (Algorithm 1) starts with the input set  $S := S_{\text{init}}$  and iteratively grows  $S$  until further growth is not possible or is not beneficial. This set  $S$  during any iteration of A\*-GCS will always be a cut-set. A\*-GCS keeps track of the growth of  $S$  in two phases (*Phase 1* and *Phase 2*). The phases are determined based on the presence of the destination in the neighborhood of  $S$ .

In *Phase 1*,  $d$  is not a member of the neighborhood of  $S$  (line 16 of Algorithm 1). Therefore, in this phase, we can find lower bounds by solving the relaxation (line 18 of Algorithm 1), but we cannot convert a relaxed solution to a feasible solution for SPP-GCS. Additionally, we add a vertex  $v \in S'$  to  $S$  if any edge  $(u, v)$  leaving  $S$  has  $y_{uv} > 0$  (line 20 of Algorithm 1, Algorithm 3).

In *Phase 2*,  $d$  is part of the neighborhood of  $S$ , and therefore, it is possible to use the relaxation to find a lower bound and a corresponding feasible solution for SPP-GCS (lines 23-24, 33-34 of Algorithm 1). During this phase, we expand  $S$  until one of the following two termination conditions is met: 1) all the vertices in  $V \setminus \{d\}$  have already been added to  $S$ , or, effectively in this condition,  $S$  cannot grow any further (line 25 of Algorithm 1), 2) the relaxation cost of traveling through any vertex in  $S' := N_S \setminus \{d\}$  becomes greater than or equal to the relaxation cost of traveling directly to  $d$ , or, effectively in this condition, growing  $S$  further may not lead to better lower bounds (line 29 of Algorithm 1). Also, the subroutine for expanding  $S$  in *Phase 2* (line 32 of Algorithm 1) mirrors that of *Phase 1*.

The following are the *key features* of A\*-GCS:

- The initial set  $S_{\text{init}}$  can be any subset of  $V$  as long as it is a cut-set. Specifically,  $S_{\text{init}}$  can either consist solely of the origin (similar to how we initiate A\* for the SPP) or be generated by an algorithm. In this paper, we also consider  $S_{\text{init}}$  generated by A\* as follows: Suppose  $\bar{S}_{A^*}$  is the closed set (which also includes  $d$ , the last vertex added to  $\bar{S}_{A^*}$ ) found by A\* when implemented on the centroids of all the convex sets associated with the vertices in  $V$ ; let  $S_{A^*} := \bar{S}_{A^*} \setminus d$  and then assign  $S_{\text{init}} := S_{A^*}$ .
- A\*-GCS can also be preemptively stopped at the end of any iteration. A\*-GCS will always produce a lower bound at the end of any iteration in any phase and may produce a feasible solution during an iteration if  $S$  is processed in *Phase 2*.
- The algorithms for updating the set (Algorithm 3) and the feasible solution (Algorithm 4) based on the fractional values of the relaxed solutions are user-modifiable. Therefore, different variants of A\*-GCS can be developed tailored to specific applications.

**Remark 3.** *A\*-GCS initiated with  $S := \{s\}$  mimics A\* in the special case when each of the convex sets is a singleton. Refer to Sec. VIII-A in the appendix for more details.*

---

**Algorithm 1:  $A^*$ -GCS**

---

```
1 Inputs:
2  $G = (V, E)$  // Input graph
3  $s, d \in V$  // Origin and destination
   vertices
4  $\mathcal{X}_u \forall u \in V$  // Input convex sets
5  $h(v) \forall v \in V$  // admissible lower bounds
6  $S_{\text{init}} \subset V$  such that  $s \in S_{\text{init}}, d \notin S_{\text{init}}$  // Input
   subset of vertices
7 Output:
8  $C_{lb}$  // Lower bound for SPP-GCS
9  $Sol_f$  // Feasible solution for SPP-GCS
10 Initialization:
11  $S \leftarrow S_{\text{init}}$ 
12  $C_{lb} \leftarrow 0$ 
13  $Sol_f \leftarrow NULL$ 
14 Main Loop:
15 Phase 1
16 while  $d \notin N_S$  do
17    $S' \leftarrow N_S$ 
18    $R_{opt}^*(S, S'), \mathcal{F}_{nd}^* \leftarrow \text{SolveRelaxation}(S, S')$ 
19    $C_{lb} \leftarrow \max(C_{lb}, R_{opt}^*(S, S'))$ 
20    $S \leftarrow \text{UpdateSubset}(S, S', \mathcal{F}_{nd}^*)$ 
21 end
22 Phase 2
23  $R_{opt}^*(S, \{d\}), \mathcal{F}_d^* \leftarrow \text{SolveRelaxation}(S, \{d\})$ 
24  $Sol_f \leftarrow \text{UpdateFeasibleSol}(Sol_f, \mathcal{F}_d^*)$ 
25 while  $\{d\} \neq N_S$  do
26    $S' \leftarrow N_S \setminus \{d\}$ 
27    $R_{opt}^*(S, S'), \mathcal{F}_{nd}^* \leftarrow \text{SolveRelaxation}(S, S')$ 
28    $C_{lb} \leftarrow \max(C_{lb}, \min(R_{opt}^*(S, S'), R_{opt}^*(S, \{d\})))$ 
29   if  $R_{opt}^*(S, S') \geq R_{opt}^*(S, \{d\})$  then
30     break
31   else
32      $S \leftarrow \text{UpdateSubset}(S, S', \mathcal{F}_{nd}^*)$ 
33      $R_{opt}^*(S, \{d\}), \mathcal{F}_d^* \leftarrow \text{SolveRelaxation}(S, \{d\})$ 
34      $Sol_f \leftarrow \text{UpdateFeasibleSol}(Sol_f, \mathcal{F}_d^*)$ 
35   end
36 end
37 return  $C_{lb}, Sol_f$ 
```

---

**Remark 4.** While  $A^*$ -GCS can be used to generate both bounds and feasible solutions, in this paper, we use  $A^*$ -GCS to primarily find bounds. Also, we generate feasible solutions using the following two-step heuristic which performs reliably well for SPP-GCS: 1) Given any convex set, choose its centroid as its representative point, and run  $A^*$  on  $(V, E)$  with the chosen points to find a path  $\mathcal{P}_{A^*}$ . 2) Let  $S := V \setminus \{d\}$  and assign  $y_{uv} = 1$  for each edge  $(u, v) \in \mathcal{P}_{A^*}$  in the formulation (1)-(8). Solve the resulting convex program to obtain the point corresponding to each vertex visited by  $\mathcal{P}_{A^*}$ .

## V. THEORETICAL RESULTS

We will first demonstrate the termination of  $A^*$ -GCS in a finite number of iterations and subsequently establish the

---

**Algorithm 2: SolveRelaxation( $S, S'$ )**

---

```
1 Solve the relaxation in (18) given  $S$  and  $S'$ 
2  $R_{opt}^*(S, S') \leftarrow$  Optimal relaxation cost
3  $\mathcal{F}^* \leftarrow$  Optimal solution to the relaxation
4 return  $R_{opt}^*(S, S'), \mathcal{F}^*$ 
```

---

---

**Algorithm 3: UpdateSubset( $S, S', \mathcal{F}_{nd}^*$ )**

---

```
// For any  $(u, v) \in \overline{E}$ , let the optimal
   value of  $y_{uv}$  in  $\mathcal{F}_{nd}^*$  be  $y_{uv}^*$ .
1  $O_S \leftarrow \{v : u \in S, v \in S', y_{uv}^* > 0\}$ 
2  $S \leftarrow S \cup O_S$ 
3 return  $S$ 
```

---

---

**Algorithm 4: UpdateFeasible( $Sol_f, \mathcal{F}_d^*$ )**

---

```
1 Use algorithms such as randomized rounding [4] to
   convert  $\mathcal{F}_d^*$  into a feasible solution,  $Sol_f^*$ , for
   SPP-GCS
2 if  $\text{Cost}(Sol_f^*) < \text{Cost}(Sol_f)$  then
3    $Sol_f \leftarrow Sol_f^*$ 
4 end
5 return  $Sol_f$ 
```

---

validity of the bounds it generates. Without loss of generality, we assume there is at least one path from  $s$  to  $d$  in the input graph  $G = (V, E)$ . This assumption helps avoid certain trivial corner cases that may arise when updating the subsets (lines 20, 32 of Algorithm 1) or the bounds (lines 19, 28 of Algorithm 1).

**Lemma 3.**  $A^*$ -GCS will terminate after completing at most  $|V| - 1$  iterations of both Phase 1 and Phase 2.

*Proof:* If the algorithm enters Phase 1, each iteration of the phase must add at least one vertex from  $N_S$  to  $S$  since there is at least one edge  $(u, v)$  leaving  $S$  such that  $y_{uv} > 0$ . If the algorithm enters Phase 2 and the termination condition in 29 is not met,  $R_{opt}^*(S, S')$  is some finite value, and therefore, there is at least one edge  $(u, v)$  leaving  $S$  and entering  $S'$  such that  $y_{uv} > 0$ . In both the phases, at most  $|V| - 1$  vertices can be added to  $S$  before at least one of the termination conditions (lines 25, 29 of Algorithm 1) become valid. Hence proved. ■

**Lemma 4.** Consider any subset  $S \subset V$  such that  $s \in S$  and  $d \notin S$ . Let the path in an optimal solution to the SPP-GCS be denoted as  $\mathcal{P}^* := (v_1^* = s, v_2^*, \dots, v_k^* = d)$  and let the optimal points in the corresponding convex sets be denoted as  $x_{v_i^*}, i = 1, \dots, k$ . For some  $p \in \{2, \dots, k\}$ , let  $v_p^*$  be such that  $v_i^* \in S$  for  $i = 1, \dots, p - 1$  and  $v_p^* \in N_S$ . Let  $S'$  be any subset of  $N_S$  that contains  $v_p^*$ . Then, the optimal cost of the SPP-GCS is at least equal to the optimal relaxation cost of SPP\*-GCS defined on  $S$  and  $S'$ , i.e.,  $C_{opt}(s, d) \geq R_{opt}^*(S, S')$ .

*Proof:* Now, the cost of the given optimal solution to SPP-GCS is:

$$\begin{aligned}
C_{opt}(s, d) &= \sum_{i=1}^{k-1} \text{cost}(x_{v_i^*}, x_{v_{i+1}^*}) \\
&= \sum_{i=1}^{p-1} \text{cost}(x_{v_i^*}, x_{v_{i+1}^*}) + \sum_{i=p}^{k-1} \text{cost}(x_{v_i^*}, x_{v_{i+1}^*}) \\
&\geq \sum_{i=1}^{p-1} \text{cost}(x_{v_i^*}, x_{v_{i+1}^*}) + h(v_p^*). \quad (\text{since } h(v_p^*) \text{ is admissible})
\end{aligned} \tag{19}$$

Now, note that the path  $(v_1^* = s, v_2^*, \dots, v_p^*)$  and the points in the corresponding convex sets  $x_{v_i^*}, i = 1, \dots, p$  is a feasible solution to SPP\*-GCS defined on  $S$  and  $S'$ . Therefore, the equation above (19) further reduces to  $C_{opt}(s, d) \geq C_{opt}^*(S, S') \geq R_{opt}^*(S, S')$ . Hence proved. ■

**Theorem 1.** Consider any subset  $S \subset V$  such that  $s \in S$  and  $d \notin S$ . Then, the optimal cost of SPP-GCS is at least equal to the optimal relaxation cost of SPP\*-GCS defined on  $S$  and  $S' := N_S$ , i.e.,  $C_{opt}(s, d) \geq R_{opt}^*(S, N_S)$ . In other words,  $R_{opt}^*(S, N_S)$  is a valid lower bound to the optimal cost of SPP-GCS.

*Proof:* This theorem follows by applying Lemma 4 with  $S' := N(S)$ . Hence proved. ■

**Theorem 2.** Consider any subset  $S \subset V$  such that  $s \in S$  and  $d \in N_S$ . Then, the optimal cost of SPP-GCS is either at least equal to the optimal relaxation cost of SPP\*-GCS defined on  $S$  and  $S' := N_S \setminus \{d\}$  or at least equal to the optimal relaxation cost of SPP\*-GCS defined on  $S$  and  $S' := \{d\}$ , i.e.,  $C_{opt}(s, d) \geq \min(R_{opt}^*(S, N_S \setminus \{d\}), R_{opt}^*(S, \{d\}))$ . In other words,  $\min(R_{opt}^*(S, N_S \setminus \{d\}), R_{opt}^*(S, \{d\}))$  is a valid lower bound to the optimal cost of SPP-GCS.

*Proof:* Consider the edge  $(v_{p-1}^*, v_p^*)$  in the optimal path in Lemma 4 that leaves  $S$  for the first time. Either  $v_p^* = d$  or  $v_p^* \in N_S \setminus \{d\}$ . If  $v_p^* = d$ , then applying Lemma 4 for  $S' = \{d\}$  leads to  $C_{opt}(s, d) \geq R_{opt}^*(S, \{d\})$ . On the other hand, if  $v_p^* \in N_S \setminus \{d\}$ , then applying Lemma 4 for  $S' = N_S \setminus \{d\}$  leads to  $C_{opt}(s, d) \geq R_{opt}^*(S, N_S \setminus \{d\})$ . Therefore,  $C_{opt}(s, d) \geq \min(R_{opt}^*(S, \{d\}), R_{opt}^*(S, N_S \setminus \{d\}))$ . Hence, proved. ■

**Remark 5.** Theorems 1 and 2 show the validity of the bounds generated by  $A^*$ -GCS. Theorem 2 also indicates why we stop growing the set  $S$  when  $R_{opt}^*(S, N_S \setminus \{d\}) \geq R_{opt}^*(S, \{d\})$ ; we assume that expanding  $S$  further without  $d$  may not result in bounds better than  $R_{opt}^*(S, \{d\})$ . However, this depends on the properties (admissibility, consistency) of the heuristic estimates. Even if  $R_{opt}^*(S, N_S \setminus \{d\}) \geq R_{opt}^*(S, \{d\})$ , it is still possible that there exists a set  $\bar{S} \subseteq V \setminus \{d\}$ ,  $\bar{S} \supset S$  such that  $R_{opt}^*(\bar{S}, N_{\bar{S}}) > R_{opt}^*(S, \{d\})$ , in which case,  $\bar{S}$  will provide better bounds. We will postpone this direction of research for future work.

## VI. NUMERICAL RESULTS

**Set up:** We initially test our algorithms on six 2D maps generated from mazes and axis-aligned bars (Fig. 3). To generate a GCS corresponding to a maze, we first partition its free space into unit squares and consider the obstacle-free sides

shared by any two adjacent squares as vertices in our GCS. The convex sets here are the line segments corresponding to the shared sides. Two vertices (or shared sides) in a maze-GCS are connected by an edge if the shared sides belong to the same unit square. An example of a GCS corresponding to a maze is shown in Fig. 3a. In the case of an instance with randomly generated, axis-aligned bars, we partition all the bars into unit squares and connect any two unit squares with an edge if they both belong to the same bar. Here, the convex sets are square regions, and an example of a GCS corresponding to a map with bars is shown in Fig. 3b. The size of the GCS generated for each of the maps is provided in Table I. The destination for each instance is always chosen to be the centroid of the top-rightmost square in the instance.

TABLE I: 2D instances generated from mazes and bars.

Map No.	Type	$ V $	$ E $
1	Maze	121	425
2	Maze	415	1020
3	Maze	1615	3649
4	Maze	6417	14239
5	Bars	769	6525
6	Bars	1790	15912

We will compare the performance of the lower bounds generated by  $A^*$ -GCS with the lower bound generated by the baseline algorithm that solves the convex relaxation of SPP-GCS on the entire graph. The upper bound<sup>3</sup> for both algorithms is the length of the feasible solution generated by the two-step heuristic. Note that the size of the cut-set during any iteration of  $A^*$ -GCS determines the sizes of the convex relaxations we will solve. Therefore, we will keep track of the sizes of the cut-sets in addition to the run times of the algorithms. Also, the baseline is equivalent to implementing (18) with  $S := V \setminus \{d\}$ ; therefore, the size of the cut-set corresponding to the baseline is  $|V| - 1$ . All the algorithms were implemented using the Julia programming language [14] and run on an Intel Haswell 2.6 GHz, 32 GB, 20-core machine. Gurobi [9] was used to solve all the convex relaxations.

**Heuristics for generating underestimates:** We designed two heuristics to generate underestimates for  $A^*$ -GCS. Given a set, the first heuristic ( $h_1$ ) simply computes the shortest Euclidean distance between any point in the set and the destination, ignoring all other vertices/edges in the graph.  $h_1$  is very fast and requires negligible computation time; it is by default present in  $A^*$ -GCS and is already part of all the run times reported in the results section. While  $h_1$  produces consistent underestimates, its bounds may not be strong.

Our second heuristic ( $h_2$ ), referred to as the *expand and freeze* heuristic, computes underestimates of the optimum through an iterative process. It starts from the destination and proceeds in the reverse direction, adding a subset of vertices  $U$  in each iteration to the set containing the destination while

<sup>3</sup>We did not use the rounding heuristic in [4] to generate upper bounds because its performance, especially for maps 5, 6, and the larger 2D and 3D maps, was significantly worse compared to the bounds produced by the two-step heuristic.

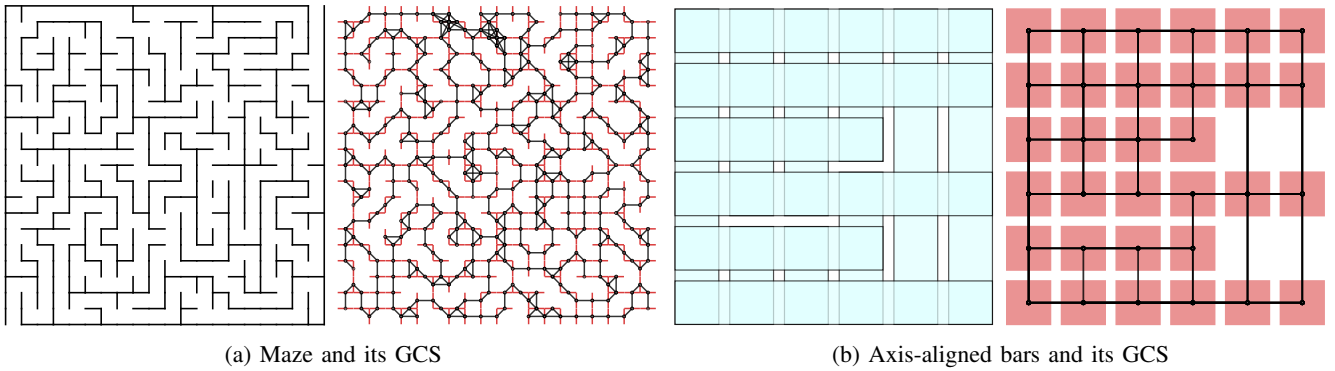


Fig. 3: 2D maps and their GCS. In the GCS corresponding to the Maze, the red segments show the convex sets and the black lines show the edges present in GCS. Similarly, in the GCS corresponding to the axis-aligned bars, the shaded squares show the convex sets and the black lines show the edges present in the GCS. Note that some edges in (b) overlap with each other.

determining the underestimate for each vertex in  $U$ . Specifically, in each iteration, the subset  $U$  and its corresponding underestimates are obtained by solving a convex relaxation of SPP\*-GCS. Any vertex that is incident to any fraction of an edge in the relaxed solution is included in  $U$ . To limit the size of the relaxations, as soon as the size of the set containing the destination reaches a limit (say  $n_{max}$ ), we shrink all the vertices in the set into a new destination vertex and repeat the process until all the (reachable) vertices are visited. In this paper, we set  $n_{max}$  as 100. Generally, for our maps,  $h_2$  produced tighter estimates than  $h_1$ , but  $h_2$  can be inconsistent<sup>4</sup>.  $h_2$  can run either in the order of seconds or minutes, depending on the map. We specify its computation times for all the maps in each of the results sections. We also study the impact of using a convex combination of the two heuristics, *i.e.*, for any vertex  $v \in V$ , we define the combined heuristic estimate as  $h(v) := (1 - w)h_1(v) + wh_2(v)$  where  $w$  is the weighting factor.

**Comparisons based on number of iterations and the sizes of the cut-sets for  $A^*$ -GCS variants:** We compare the performance of  $A^*$ -GCS for two choices of  $S_{init}$ : one with  $S_{init} := \{s\}$  and another with  $S_{init} := S_{A^*}$  (refer to the key features of  $A^*$ -GCS on page 4). We fix the origin for each map in Table I at the centroid of the left-bottommost unit square and implement the variants of  $A^*$ -GCS on the corresponding graphs for heuristic weight  $w = 1$ . The bounds produced by both the choices of  $S_{init}$  are the same for these six maps. Therefore, for both the variants, we compare the total number of iterations for both phases of  $A^*$ -GCS, the size of the cut-set ( $|S|$ ) upon termination of  $A^*$ -GCS, and the total run time (in secs.) as shown in Table II. While  $|S|$  for both variants of  $A^*$ -GCS are relatively closer,  $A^*$ -GCS initialized with  $S_{init} := \{s\}$  required significantly more iterations and run time to terminate compared to the  $A^*$ -GCS initialized with  $S_{init} := S_{A^*}$ . This trend remained the same for any other choice of origin in these maps. Therefore, for the remaining results in this paper, we will only focus on the variant of  $A^*$ -

GCS initialized with  $S_{init} := S_{A^*}$ . Note that in this variant, the algorithm will never enter Phase 1 since the destination  $d$  is already present in the neighborhood of  $S_{A^*}$ . Henceforth, the number of iterations of  $A^*$ -GCS will simply refer to the number of iterations in Phase 2 of  $A^*$ -GCS.

TABLE II: No. of iterations ( $n_{iter}$ ), the size of the cut-set ( $|S|$ ) upon termination and the run time (in secs.) for the  $A^*$ -GCS variants.

Map No.	$S_{init} := \{s\}$			$S_{init} := S_{A^*}$		
	$n_{iter}$	$ S $	time	$n_{iter}$	$ S $	time
1	27	36	0.23	3	44	0.07
2	117	149	3.4	1	196	0.1
3	383	422	43.98	2	518	0.69
4	1726	2699	1077.99	2	4003	4.48
5	110	585	126.3	1	654	2.8
6	171	1657	962.94	1	1693	24.06

TABLE III: Heuristic  $h_2$  run time in secs.

Map No.					
1	2	3	4	5	6
14.40	21.50	48.41	151.68	43.27	94.40

**Impact of the quality of underestimates:** For each map in Table I, we generated 100 instances, with each instance choosing a different origin for the path. The run times for heuristic  $h_2$  are shown in Table III. Note that this heuristic is run only once and is used as an input for all the 100 instances for any heuristic weight  $w > 0$ . Given an instance  $I$ , its optimality gap is defined as  $100 \times \frac{C_f - C_{ib}}{C_{ib}}$ , where  $C_f$  is the length of the feasible solution obtained by the two-step algorithm in Remark 4, and  $C_{ib}$  is the bound returned by  $A^*$ -GCS. In Table IV, we present the results (average size of cut-sets, average run times in seconds, and the average optimality gap) at the end of the first iteration of  $A^*$ -GCS (referred to as  $A^*$ -GCS<sub>1</sub>) as well as upon the termination of  $A^*$ -GCS (referred to as  $A^*$ -GCS<sub>∞</sub>). Even with a heuristic weight  $w = 0$  (which corresponds to the first heuristic  $h_1$  that provides relatively weak bounds),  $A^*$ -GCS is able to

<sup>4</sup>Note that developing fast and efficient heuristics is an art in itself and the influence of their properties (admissibility and consistency) on the ensuing search process is a non-trivial [15], [16] exercise even for well studied SPPs. Since SPP-GCS is a relatively new problem, future work can consider the development of fast and efficient heuristics for SPP-GCS.

TABLE IV: Average size of the cut-set ( $|S|$ ), average run times (in secs) and average optimality gap (in %) for different levels of heuristic weights for maps in Table I.

Map No.	Algorithm	$w = 0$			$w = 0.25$			$w = 0.5$			$w = 0.75$			$w = 1.0$		
		$ S $	time	gap	$ S $	time	gap	$ S $	time	gap	$ S $	time	gap	$ S $	time	gap
1	Baseline	120.0	0.1	0.1	120.0	0.1	0.1	120.0	0.1	0.1	120.0	0.1	0.1	120.0	0.1	0.1
	$A^*-GCS_\infty$	37.3	0.1	0.1	35.4	0.1	0.1	32.8	0.0	0.1	31.1	0.0	0.1	30.4	0.0	0.1
	$A^*-GCS_1$	36.1	0.0	3.4	34.1	0.0	3.4	31.6	0.0	3.4	29.8	0.0	3.4	28.9	0.0	3.4
2	Baseline	414.0	0.4	0.3	414.0	0.4	0.3	414.0	0.4	0.3	414.0	0.3	0.3	414.0	0.3	0.3
	$A^*-GCS_\infty$	225.9	0.2	0.3	201.2	0.2	0.3	174.5	0.1	0.3	151.3	0.1	0.3	123.9	0.1	0.3
	$A^*-GCS_1$	225.9	0.2	0.5	201.2	0.1	0.4	174.5	0.1	0.3	151.2	0.1	0.4	123.9	0.1	0.3
3	Baseline	1614.0	1.0	0.0	1614.0	1.0	0.0	1614.0	1.0	0.0	1614.0	1.0	0.0	1614.0	1.0	0.0
	$A^*-GCS_\infty$	683.6	1.0	0.0	610.5	0.8	0.0	531.5	0.7	0.0	467.1	0.6	0.0	402.9	0.5	0.0
	$A^*-GCS_1$	683.6	0.5	0.3	610.5	0.4	0.2	531.5	0.3	0.1	467.1	0.3	0.1	402.9	0.2	0.1
4	Baseline	6416.0	5.9	0.0	6416.0	5.9	0.0	6416.0	5.9	0.0	6416.0	5.8	0.0	6416.0	5.9	0.0
	$A^*-GCS_\infty$	2858.2	3.4	0.0	2575.9	3.0	0.0	2309.3	2.7	0.0	2054.3	2.3	0.0	1786.8	1.9	0.0
	$A^*-GCS_1$	2858.2	1.7	0.0	2575.9	1.4	0.0	2309.3	1.3	0.0	2054.3	1.1	0.0	1786.8	1.0	0.0
5	Baseline	768.0	3.8	2.6	768.0	3.8	2.6	768.0	3.9	2.6	768.0	3.9	2.6	768.0	3.8	2.6
	$A^*-GCS_\infty$	343.9	2.8	2.6	314.6	2.5	2.6	291.7	2.1	2.5	265.3	1.8	2.6	241.2	1.3	2.6
	$A^*-GCS_1$	340.9	1.4	3.3	312.8	1.3	3.4	290.3	1.2	3.0	264.6	1.2	3.0	240.5	1.0	2.8
6	Baseline	1789.0	20.5	2.4	1789.0	20.6	2.4	1789.0	20.5	2.4	1789.0	20.6	2.4	1789.0	20.6	2.4
	$A^*-GCS_\infty$	911.2	24.0	2.4	809.3	19.4	2.4	713.3	13.3	2.4	616.8	10.2	2.4	515.1	6.4	2.4
	$A^*-GCS_1$	882.9	9.4	4.5	788.4	7.1	3.9	694.4	6.0	3.7	601.2	3.6	4.2	508.7	2.8	2.9

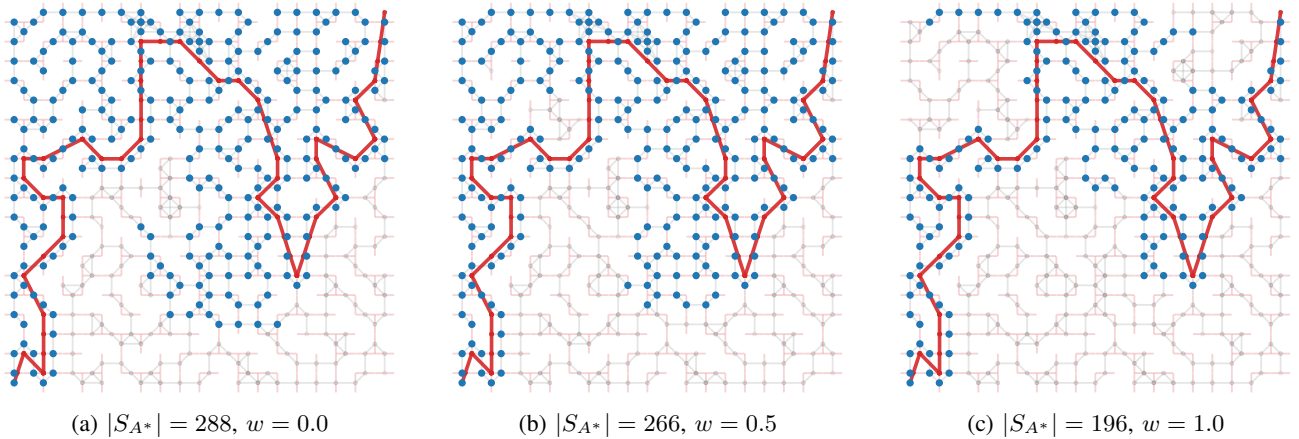


Fig. 4: The feasible path (shown using thick red lines) and the cut-set vertices (shown in color blue) produced by the two-step  $A^*$  based heuristic for different weights. There are 415 vertices in this GCS corresponding to map no. 2.  $A^*-GCS$  applied on this instance terminates in 1 iteration for all the heuristic weights. By first finding the cut-set ( $S_{A^*}$ ) and then applying  $A^*-GCS$  with  $S_{init} := S_{A^*}$ , we reduced the size of the convex relaxation corresponding to  $|V| - 1 = 414$  vertices into a convex relaxation corresponding to  $|S_{A^*}|$  vertices.

reduce the size of the cut-sets (which, in turn, *reduces the sizes of convex relaxations to solve*) by more than 45%, on average (except in map no. 6). In fact, by selecting the cut-set informed by  $A^*$  with  $w = 0$  and completing just one iteration of  $A^*-GCS$ , we achieve optimality gaps in a shorter time that closely match those provided by the baseline algorithm (except for map no. 6). Refer to Fig. 4 for an illustration. For map no. 6 the underestimates provided by  $h_1$  was much weaker compared to  $h_2$ , and hence  $A^*-GCS$  performed significantly better when the heuristic weight was increased to 1.

For single query problems, the results for the 2D maps show that the default heuristic ( $h_1$ ) in  $A^*-GCS$  is sufficient to provide benefits in terms of reduction in problem sizes and computation time. On the other hand, for multi-query problems, using  $h_2$  can further significantly reduce the computation time while providing similar optimality gaps. For example, in map no. 6,  $A^*-GCS_1$  is at least six times faster

than the baseline algorithm for  $w = 1$ .  $A^*-GCS$  performed the best in map no. 4 for all heuristic weights; specifically,  $A^*-GCS_1$  found optimal solutions with average run times considerably lower compared to the baseline for this map. As the heuristic weight increased, the size of the cut-sets as well as the run times decreased on average; however, this trend may not always hold (refer to Sec. VIII-B in the appendix).

**$A^*-GCS$  on a large 2D map:**  $A^*-GCS$  was next tested on a large 2D maze with its corresponding GCS containing 25,615 vertices and 56,550 edges. Similar to the previous runs, we generated 100 instances for this map, varying the origins of the paths. For all the instances,  $A^*-GCS$  terminated in just one iteration for all the heuristic weights and produced optimal solutions. Specifically,  $A^*-GCS$  with the default heuristic ( $h_1$ ) outperformed the baseline both in terms of reduced problem sizes (cut-sets) and run time by more than 50% (Fig. 5). Heuristic  $h_2$  required 330.25 secs to compute for this map.

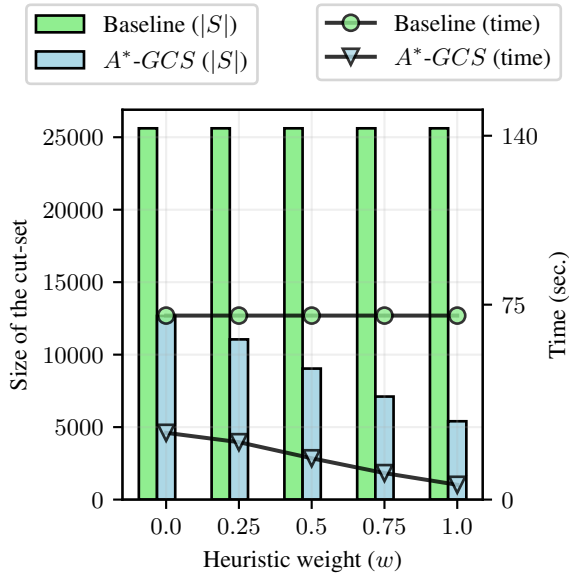


Fig. 5: Average cut-set sizes and run times (in secs.) for a large 2D map. Both the algorithms found the optimal solutions for all the instances in this map.

In a multi-query setting, using  $A^*$ -GCS with  $h_2$  can further provide significant benefits as seen in Fig. 5.

#### $A^*$ -GCS on large 3D village maps:

Finally,  $A^*$ -GCS was applied to two large 3D village maps (Fig. 6) created using the meshcat library in Python. We followed a procedure similar to the one described for maps in Table I to develop the GCS for these village maps. The convex sets in these maps, resulting from the intersection of adjacent cubes, are axis-aligned squares (shared sides of adjacent cubes) computed using the algorithm in [17]. The GCS corresponding to the first 3D map has 6010 vertices and 166,992 edges, while the GCS for the second 3D map has 11,258 vertices and 321,603 edges. In both maps, the origin and destination were chosen at opposite corners of the 3D region. The computation time for heuristic  $h_2$  for these two maps was 53.30 secs and 89.10 secs respectively.

The baseline algorithm for the first 3D map required 1848 seconds to solve with an optimality gap of 12.56%. The optimality gaps obtained after each iteration of  $A^*$ -GCS and their corresponding run times are shown in Fig. 7. *The key insight from this figure is that  $A^*$ -GCS, after one iteration, is able to achieve an optimality gap of around 15.5% in less than 300 seconds for heuristic weight  $w = 0$  (corresponding to the heuristic  $h_1$ ).* Note that running  $A^*$ -GCS to termination may not be helpful in this map, as the run times per iteration are relatively high; therefore, for heuristic weight  $w = 0$ ,  $A^*$ -GCS requires around 2000 seconds to terminate. Even if one adds the  $h_2$  computation time (53.3 secs) to the run time for any weight  $> 0$ ,  $A^*$ -GCS<sub>1</sub> outperforms the baseline in terms of run times while providing similar optimality gaps.

The results for the second 3D map are presented in Table V, with  $A^*$ -GCS terminating after just one iteration for all the heuristic weights (except for  $w = 0$  which required 2 iterations). Again, even if the heuristic  $h_2$  computation time

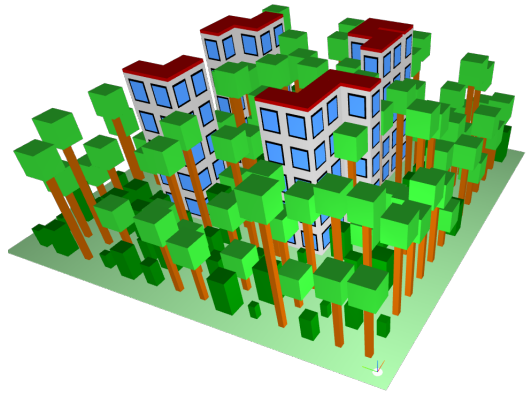


Fig. 6: 3D village map.

(89.10 secs) is added to the run times in Table V,  $A^*$ -GCS for any  $w > 0$ , finds solutions of similar quality significantly faster than the baseline.

TABLE V: Results for the second 3D map: Size of the cut-set ( $|S|$ ), run time (in secs.) and optimality gap (in %).

$w$		Baseline	$A^*$ -GCS
0	$ S $	11257	11257
	time	1847.4	1335.2
	gap	9.18	8.74
0.25	$ S $	11257	11257
	time	1847.4	653.5
	gap	9.18	8.85
0.5	$ S $	11257	11257
	time	1847.4	820.3
	gap	9.18	9.06
0.75	$ S $	11257	10873
	time	1847.4	811.7
	gap	9.18	9.06
1	$ S $	11257	7676
	time	1847.4	824.5
	gap	9.18	9.06

## VII. CONCLUSIONS AND FUTURE WORK

In this paper, we show how to combine the existing convex-programming based approach with heuristic information to obtain near-optimal solutions for SPP-GCS. For Euclidean travel costs, we demonstrate that finding a feasible solution first using  $A^*$  and then solving a convex relaxation on the subset of vertices informed by  $A^*$  can reduce the size of the problems solved and computation times. There are several research directions for this work. One useful direction is to develop fast and consistent heuristics that can provide good underestimates for the SPP-GCS\*. As mentioned in Remark 5, it would be useful to further understand the relationship between the properties of the underestimates (admissibility, consistency) and the bounds generated by  $A^*$ -GCS. For large graphs, there are differential and compressed differential heuristics [18], [19] available for the SPP. Similar heuristic development for SPP-GCS can also be advantageous.  $A^*$ -GCS can be considered as a uni-directional search method where the sets grow from the origin only in one direction

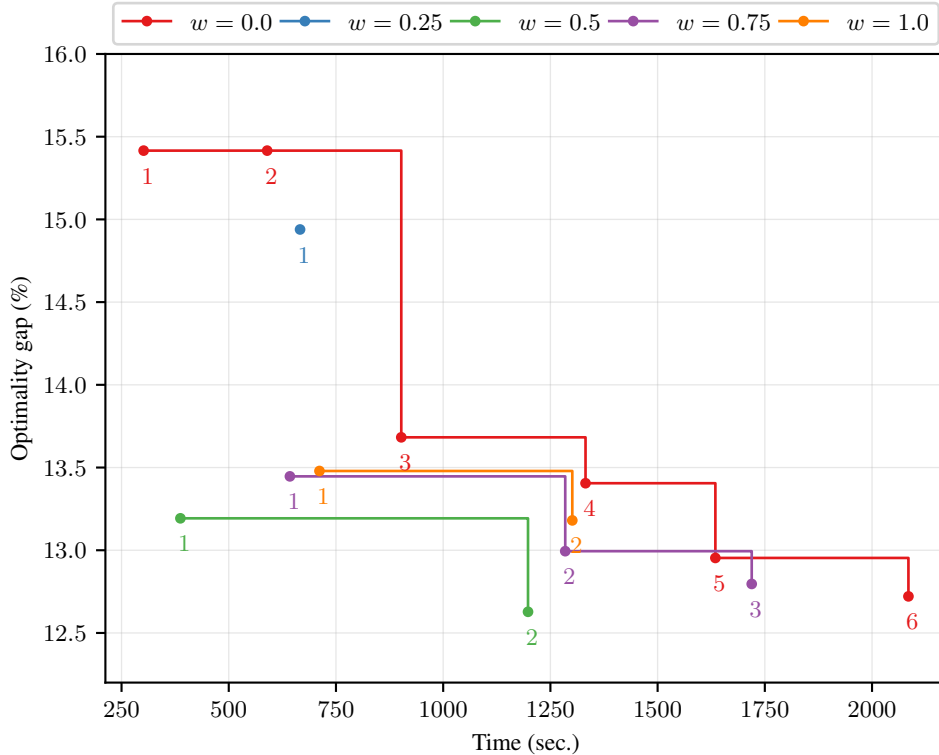


Fig. 7: Results for the first 3D map: the optimality gap (%) and run times (in secs) obtained after each iteration of  $A^*$ -GCS with varying heuristic weights. The numbers marked next to the lines indicate when each of the iterations of  $A^*$ -GCS completed. The baseline algorithm required 1848 seconds to compute a lower bound for this map with an optimality gap of 12.56%.

towards the destination. Bi-directional variants of  $A^*$ -GCS, just like the ones available for the SPP [20], [21], also have the potential to speed up the search process. Finally, for the scope of this paper, we exclusively considered the Euclidean distance metric. Subsequent work can explore extensions of our approach to other distance or time or energy based metrics.

## REFERENCES

- [1] E. L. Lawler, "Shortest path and network flow algorithms," in *Discrete Optimization I* (P. Hammer, E. Johnson, and B. Korte, eds.), vol. 4 of *Annals of Discrete Mathematics*, pp. 251–263, Elsevier, 1979.
- [2] B. Korte and J. Vygen, *Shortest Paths*, pp. 159–175. Berlin, Heidelberg: Springer Berlin Heidelberg, 2018.
- [3] A. Madkour, W. G. Aref, F. U. Rehman, M. A. Rahman, and S. Basalamah, "A survey of shortest-path algorithms," *arXiv*, 2017.
- [4] T. Marcucci, J. Umenberger, P. A. Parrilo, and R. Tedrake, "Shortest paths in graphs of convex sets," *CoRR*, vol. abs/2101.11565, 2021.
- [5] T. Marcucci, M. Petersen, D. von Wrangel, and R. Tedrake, "Motion planning around obstacles with convex optimization," *Science Robotics*, vol. 8, no. 84, p. eadf7843, 2023.
- [6] T. Marcucci, P. Nobel, R. Tedrake, and S. Boyd, "Fast path planning through large collections of safe boxes," *arXiv*, 2023.
- [7] E. M. Arkin and R. Hassin, "Approximation algorithms for the geometric covering salesman problem," *Discrete Applied Mathematics*, vol. 55, no. 3, pp. 197–218, 1994.
- [8] A. Dumitrescu and J. S. Mitchell, "Approximation algorithms for tsp with neighborhoods in the plane," *Journal of Algorithms*, vol. 48, no. 1, pp. 135–159, 2003.
- [9] Gurobi Optimization, LLC, "Gurobi Optimizer Reference Manual," 2023.
- [10] J. Canny and J. Reif, "New lower bound techniques for robot motion planning problems," in *28th Annual Symposium on Foundations of Computer Science (sfcs 1987)*, pp. 49–60, 1987.
- [11] J. S. B. Mitchell, *Shortest paths and networks*, p. 445–466. USA: CRC Press, Inc., 1997.
- [12] P. E. Hart, N. J. Nilsson, and B. Raphael, "A formal basis for the heuristic determination of minimum cost paths," *IEEE Transactions on Systems Science and Cybernetics*, vol. SSC-4(2), pp. 100–107, 1968.
- [13] E. Lawler, *Combinatorial optimization - networks and matroids*. New York: Holt, Rinehart and Winston, 1976.
- [14] J. Bezanson, A. Edelman, S. Karpinski, and V. B. Shah, "Julia: A fresh approach to numerical computing," *SIAM Review*, vol. 59, no. 1, pp. 65–98, 2017.
- [15] U. Zahavi, A. Felner, J. Schaeffer, and N. Sturtevant, "Inconsistent heuristics," in *Proceedings of the 22nd National Conference on Artificial Intelligence - Volume 2, AAAI'07*, p. 1211–1216, AAAI Press, 2007.
- [16] R. Holte, "Common misconceptions concerning heuristic search," in *Proceedings of the 3rd Annual Symposium on Combinatorial Search, SoCS 2010*, 09 2010.
- [17] A. Zomorodian and H. Edelsbrunner, "Fast software for box intersections," in *Proceedings of the sixteenth annual symposium on Computational geometry*, pp. 129–138, 2000.
- [18] A. V. Goldberg and C. Harrelson, "Computing the shortest path: A search meets graph theory," in *Proceedings of the Sixteenth Annual ACM-SIAM Symposium on Discrete Algorithms*, p. 156–165, 2005.
- [19] M. Goldenberg, N. Sturtevant, A. Felner, and J. Schaeffer, "The compressed differential heuristic," in *Proceedings of the Twenty-Fifth AAAI Conference on Artificial Intelligence*, p. 24–29, 2011.
- [20] T. A. J. Nicholson, "Finding the Shortest Route between Two Points in a Network," *The Computer Journal*, vol. 9, pp. 275–280, 11 1966.
- [21] R. C. Holte, A. Felner, G. Sharon, N. R. Sturtevant, and J. Chen, "Mm: A bidirectional search algorithm that is guaranteed to meet in the middle," *Artificial Intelligence*, vol. 252, pp. 232 – 266, 2017.

## VIII. APPENDIX

### A. Special case of SPP-GCS

Assume each of the convex sets associated with the vertices in  $V$  is a singleton. Let the cost of traveling from  $u \in V$  to  $v \in V$  be denoted as  $cost_{uv} \in \mathbb{R}^+$ . Let the underestimates denoted

TABLE VI: Average sizes of cut-sets ( $|S|$ ), run times (in secs.) and optimality gap (in %) for different levels of heuristic weights.

Algorithm	$w = 0$			$w = 0.25$			$w = 0.5$			$w = 0.75$			$w = 1.0$		
	$ S $	time	gap	$ S $	time	gap	$ S $	time	gap	$ S $	time	gap	$ S $	time	gap
Baseline	1104.0	16.3	2.8	1104.0	16.1	2.8	1104.0	16.1	2.8	1104.0	16.3	2.8	1104.0	16.4	2.8
$A^*$ - $GCS_\infty$	250.7	18.0	2.6	424.7	39.0	2.7	556.6	66.0	2.7	669.9	88.7	2.7	781.6	103.6	2.8
$A^*$ - $GCS_1$	183.9	0.9	8.6	321.3	1.9	14.1	441.9	3.1	18.8	559.5	4.5	22.3	683.0	6.6	23.7

by  $h(u)$ ,  $u \in V$  be consistent, i.e.,  $h(u) \leq cost_{uv} + h(v)$  for all  $(u, v) \in E$ . In this special case, consider an implementation of  $A^*$  on  $(V, E)$  with its closed set initialized to  $\{s\}$ . Until termination, each iteration of  $A^*$  picks a vertex (say  $v^*$ ) in  $N_S$  with the least  $f$  cost<sup>5</sup> for expansion and moves  $v^*$  from  $N_S$  to  $S$ . If the underestimates are consistent, once  $v^*$  is chosen for expansion and added to  $S$ , it will never be chosen for expansion again (i.e., never removed from  $S$  again).  $A^*$  terminates when  $v^*$  is the destination. This is also how  $A^*$ - $GCS$  performs in this special case for the following reasons: From Remarks 1-2, solving the relaxations in either Phase 1 or Phase 2 of  $A^*$ - $GCS$  is equivalent to solving a shortest path problem where the objective is to choose a vertex  $v$  in  $N_S$  with the least  $f$  cost (the sum of the travel cost from  $s$  to  $v$  and  $h(v)$ ) such that the path starts from the origin, travels through the vertices in  $S$  and reaches one of the vertices in  $N_S$ . Until termination, each iteration of any of the phases in  $A^*$ - $GCS$  will move one vertex from  $N_S$  to  $S$  (based on where the shortest path ends in  $N_S$ ). In addition, if the shortest path found in Phase 2 of  $A^*$ - $GCS$  ends at the destination (or if  $R_{opt}^*(S, S') \geq R_{opt}^*(S, \{d\})$  is true),  $A^*$ - $GCS$  will terminate just like  $A^*$ .

### B. Challenging instances for $A^*$ - $GCS$

In this subsection, we present a map for which  $A^*$ - $GCS$  did not show much improvement compared to the baseline algorithm. Fig. 8 illustrates this map with randomly generated boxes used in [4]. The GCS constructed for this map has 1106 vertices and 13885 edges. We generated 100 instances with different origins, and the results for these instances are presented in Table VI. When  $w = 0$ , the average optimality gap and run time of  $A^*$ - $GCS$  upon termination with respect to the baseline were similar. After one iteration,  $A^*$ - $GCS$  obtained bounds that are around 8.6% relatively quickly, but this gap is (relatively) weaker compared to the optimality gaps we obtained for most of the other maps. Additionally, increasing the heuristic weight did not provide any benefits for this map, as the average sizes of the cut-sets as well as the total run times of  $A^*$ - $GCS$  increased (likely due to weak and inconsistent underestimates from the second heuristic). There are two ways we can address this map in future work: 1) one way is to develop better underestimates; currently, the bounds from both heuristics are not strong for this map, 2) another way is to ensure the boxes do not randomly overlap by breaking the boxes into smaller pieces, similar to the processing we implemented for maps with axis-aligned bars. Although this procedure will increase the number of vertices and edges, just

like the large 2D instances, we expect the improvements using  $A^*$ - $GCS$  to be more significant.

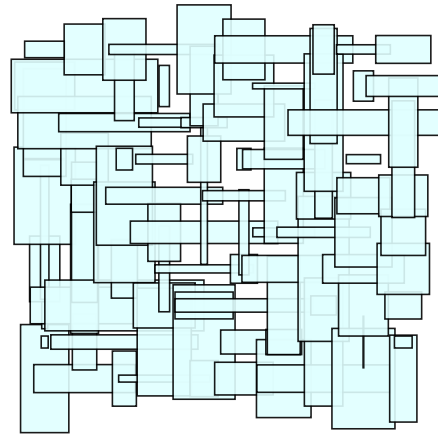


Fig. 8: Randomly generated rectangles.

<sup>5</sup>Here, we borrow the usual definition of  $f$  and  $g$  costs from  $A^*$  [12].